

Simulation of 4f–5d transitions of Yb^{2+} in potassium and sodium halides

This article has been downloaded from IOPscience. Please scroll down to see the full text article.

2008 J. Phys.: Condens. Matter 20 215228

(<http://iopscience.iop.org/0953-8984/20/21/215228>)

View [the table of contents for this issue](#), or go to the [journal homepage](#) for more

Download details:

IP Address: 129.252.86.83

The article was downloaded on 29/05/2010 at 12:28

Please note that [terms and conditions apply](#).

Simulation of 4f–5d transitions of Yb^{2+} in potassium and sodium halides

Chang-Kui Duan^{1,2} and P A Tanner²

¹ Institute of Modern Physics, Chongqing University of Post and Telecommunications, Chongqing 400065, People's Republic of China

² Department of Biology and Chemistry, City University of Hong Kong, Tat Chee Avenue, Kowloon, Hong Kong SAR, People's Republic of China

Received 26 January 2008, in final form 8 April 2008

Published 25 April 2008

Online at stacks.iop.org/JPhysCM/20/215228

Abstract

The free ion energy level parameters of Yb^{2+} are obtained by fitting the $4f^{13}5d$ Yb^{2+} free ion energy levels. A model is proposed for scaling these parameters so that they are appropriate for Yb^{2+} in crystals. Treating the scaling factor, the barycenter energy E_{exc} of the $4f^{13}5d$ configuration, and the crystal-field splitting parameter $B^4(\text{dd})$ as free parameters and adopting the 4f crystal-field parameters of the $4f^{13}$ configuration Yb^{3+} ion in other hosts with the same ligands, the absorption spectra of Yb^{2+} in MX ($M = \text{K}, \text{Na}; X = \text{F}, \text{Cl}, \text{Br}, \text{I}$) hosts are well simulated. A model is proposed for taking the effect of charge compensation into account and this shows that the inclusion of charge compensation effects does not significantly alter the calculated electronic absorption spectra but may considerably change the dynamics of the system.

1. Introduction

Studies of 4f–5d transitions of lanthanide ions have attracted great interest recently partly because of the effort to develop technological applications, such as new phosphors for lamps and displays [1–5] and short wavelength lasers. Actually, 4f–5d transitions in divalent lanthanide ions have been studied much earlier, due to the fact that the electric dipole allowed transitions are generally at lower energies than in the corresponding trivalent ions so that strong ultraviolet or visible luminescence occurs. Literature electronic spectra of Eu^{2+} , Sm^{2+} and Yb^{2+} up to 1991 have been clearly summarized by Rubio [6]. Most studies are on hosts with high symmetry (cubic), so that the structure of the spectra can be interpreted in terms of (vibronic) transitions between crystal-field energy levels.

It is well known that, due to localization of 4f orbitals, the $4f^N$ ($N = 1–14$) energy levels of a given lanthanide ion differ from host to host by only the crystal-field splittings of up to a few hundred of wavenumbers, which can be parameterized by a quasi-free ion Hamiltonian (with parameters varying in a limited range) plus a symmetry-adapted crystal-field Hamiltonian [7]. In most cases, the intraconfigurational spectra (at low temperature) are composed of well-resolved, sharp lines that correspond to transitions between 4f levels without involving phonons, which make the theoretical interpretation

and simulation of 4f–4f spectra in many cases straightforward. However, since 5d orbitals are more extended and interact more strongly with ligands, the $4f^{N-1}5d$ ($N = 1–14$) energy levels of a given lanthanide ion may be completely different in different hosts [8]. An additional complication is that interconfigurational $4f^N–4f^{N-1}5d$ transitions are in general composed of very broad peaks due to a displacement of the vibrational equilibrium position between the ground and excited states. Therefore, there are very few electronic energy levels clearly resolvable experimentally and in general there is no simple and routine interpretational method, apart from some trials using phenomenological methods to predict the onset energies [9–12] and simplified models to predict the overall structure of 4f–5d absorption [13, 14]. More sophisticated calculations based on an extended $4f^N$ Hamiltonian by including 5d spin–orbit and crystal-field interactions, and 4f–5d Coulomb interactions have also been carried out in many systems [8, 15]. The persistent problem of such a calculation is that it contains in general far more adjustable parameters than experimentally-resolved electronic levels, and many of the important parameters that involve 5d orbitals (5d crystal-field, 5d spin–orbit interaction and 4f–5d Coulomb interaction parameters) are strongly host-dependent.

More recently, we have recorded the absorption, emission and excitation spectra of $\text{Yb}^{2+}:\text{SrCl}_2$ and measured the temperature dependence of the lifetimes of $4f^{13}5d \rightarrow 4f^{14}$

Table 1. Yb²⁺ 4f¹³5d and 4f¹³6s (last 4 rows) free ion levels in cm⁻¹.

Label	Measured	Calculated	Diff
³ P ₂ (90%)	33 386	33 575	189
³ H ₅ (57%) + ¹ H ₅ (40%)	37 020	37 024	3
³ H ₆ (100%)	39 076	38 839	-236
³ D ₃ (59%) + ³ F ₃ (35%)	39 141	38 973	-169
³ P ₁ (80%)	39 721	39 722	1
³ F ₄ (47%) + ³ G ₄ (34%)	40 160	40 045	-115
¹ D ₂ (53%) + ³ D ₂ (30%)	40 288	40 575	287
³ F ₄ (45%) + ¹ G ₄ (33%)	42 425	42 523	98
¹ F ₃ (39%) + ³ D ₃ (32%)	43 019	43 061	42
³ G ₅ (84%)	43 623	43 541	-82
³ P ₀ (100%)	45 421	45 381	-40
³ H ₄ (77%)	470 57	46 971	-86
¹ D ₂ (43%) + ³ F ₂ (39%)	48 415	48 620	205
³ D ₁ (83%)	50 030	49 843	-187
¹ H ₅ (45%) + ³ H ₅ (42%)	50 358	50 382	24
³ F ₂ (48%) + ³ D ₂ (44%)	51 463	51 401	-62
³ G ₃ (60%) + ¹ F ₃ (35%)	51 582	51 517	-65
³ F ₃ (41%) + ³ G ₃ (29%)	53 123	53 179	56
¹ P ₁ (90%)	53 365	53 369	4
³ G ₄ (54%) + ¹ G ₄ (37%)	53 736	53 869	133
(4f ¹³ 7/2 6s) 4 ^a	34 656		
(4f ¹³ 7/2 6s) 3 ^a	34 990		
(4f ¹³ 5/2 6s) 2 ^a	44 854		
(4f ¹³ 5/2 6s) 3 ^a	45 208		

^a 4f¹³6s levels in the format (4f¹³ J_f 6s) J, where J_f is the total angular momentum of 4f¹³ and J is the total angular momentum of 4f¹³6s.

transitions and carried out detailed theoretical simulations of both crystal-field levels of the 4f¹³5d configuration and of luminescence dynamics [16]. We notice that the Yb²⁺ ion is very suitable for a detailed and in some cases a very definite, study of the strength of interactions involving 5d orbitals, especially in a host with high site symmetry such as O_h, because the 4f–5d absorption and 5d–4f emission are restricted to a limited number of energy levels since the ground state is a singlet spin and totally symmetric orbital state and transitions are restricted by selection rules between the crystal-field levels of certain irreducible representations.

While more detailed experimental studies are scheduled on Yb²⁺ doped in hosts of the same structure as SrCl₂, we present in this work the simulation of 4f–5d transitions of Yb²⁺ in potassium and sodium halides which were measured by Bland and Smith [17] and Tsuboi *et al* [18, 19]. In section 2 the parameters of 4f–5d Coulomb interaction, and 4f and 5d spin-orbit interactions for free Yb²⁺ ions are optimized using the recent free ion levels presented by Öberg and Lundberg [20]. In section 3 a single (adjustable) parameter model is proposed to relate the (quasi-) free ion parameters of the doped Yb²⁺ ion to the real Yb²⁺ ion, and then by treating the single crystal-field splitting of 5d orbitals with an adjustable parameter, and importing value of the 4f crystal-field parameter from the same ion in other hosts with the same ligands, the energy levels and absorption spectra of Yb²⁺ in MX (M = K, Na; X = F, Cl, Br, I) are calculated. In section 4 a model to account for the effect of charge compensation anion vacancy is proposed and its effect upon the absorption spectra and luminescence dynamics are discussed via detailed calculation.

Table 2. Parameters (in cm⁻¹) for Yb²⁺ free ion.

Parameters	Previous		Obtained in this work	
	value [17]	HF value	Value	Uncertainty
E_{exc}	44 073		44 629	175
$F^2(\text{fd})$	19 614	23 210	20 089	412
$F^4(\text{fd})$	9 868	10 646	11 250	838
$G^1(\text{fd})$	6 762	10 059	6 908	113
$G^3(\text{fd})$	7 755	8 046	8 124	988
$G^5(\text{fd})$	6 266	6 085	6 900	1093
ζ_{4f}	2 950.2	2 899	2 927	24
ζ_{5d}	1 211	1 291	1 162	37

2. Modeling of energy levels of Yb²⁺ free ion

The 4f¹³5d energy levels of Yb²⁺ free ion can be calculated with the following Hamiltonian:

$$H_{\text{fi}} = E_{\text{exc}} + \zeta_{4f} \mathbf{s}_{4f} \cdot \mathbf{l}_{4f} + \zeta_{5d} \mathbf{s}_{5d} \cdot \mathbf{l}_{5d} + \sum_{k=2,4} F^k(\text{fd}) \hat{f}_k(\text{fd}) + \sum_{k=1,3,5} G^k(\text{fd}) \hat{g}_k(\text{fd}),$$

where E_{exc} is the energy of the barycenter for the 4f¹³5d configuration relative to the ground state 4f¹⁴ ¹S₀; ζ_{4f} and ζ_{5d} are 4f and 5d spin-orbit parameters, respectively; and $F^k(\text{fd})$ and $G^k(\text{fd})$ are Slater integrals for direct and exchange Coulomb interaction between the 4f and 5d orbitals. It is noted that 4f¹³ is equivalent to one hole in the fully-filled 4f¹⁴ configuration, so that the Coulomb interaction between 4f orbitals only contributes a constant shift to the 4f¹³5d configuration that can be absorbed into E_{exc} . Öberg and Lundberg [20] have recently improved the assignment of level energies of the Yb²⁺ free ion. The energies relevant to the analysis here from the 4f¹³5d and 4f¹³6s configurations are presented in table 1 with our fitted energies for 4f¹³5d, which range from 30 000 to 55 000 cm⁻¹ relative to the single 4f¹⁴ state. The parameter values obtained are listed in table 2, which will serve as starting point for the simulation of the energy levels for Yb²⁺ ions in crystals. For comparison, values used in previous work on Yb²⁺ and from Hartree–Fock (HF) calculation [21] are also listed in table 2. It can be seen that HF values for $F^2(\text{fd})$ and $G^1(\text{fd})$ are significantly larger than the corresponding ‘experimental’ free ion values, so that the former cannot be actually treated as real free ion values. The HF values for other higher rank Coulomb interaction are almost the same as ‘experimental’ free ion values. This suggests that in energy level calculations, it is more sensible to compare the quasi-free ion parameters for Yb²⁺ in crystals with ‘experimental’ free ion values than with HF values.

3. Modeling of the energy levels and absorption spectra of Yb²⁺ in crystals

3.1. Crystal-field interactions

The 5d orbitals of lanthanide ions spread out much more than 4f orbitals, and so are subject to a much stronger crystal-field splitting (than 4f orbitals). The crystal-field parameters for a 5d electron are usually more than an order of magnitude

Table 3. Parameter values (in cm^{-1}) for Yb^{2+} in various alkali halide hosts. Values in brackets are fixed; $B_0^6(\text{ff})/B_0^4(\text{ff}) = 0.11$ is used; N is the number of measured levels and σ is the residual error of the fitting.

Parameter	E_{exc}	$B^4(\text{dd})$	$B_0^4(\text{ff})$	ζ_{4f}	η	N	σ
KF	$40\,102 \pm 87$	$34\,375 \pm 232$	[2250]	[2927]	0.804 ± 0.024	5	77
KBr	$36\,235 \pm 154$	$22\,544 \pm 305$	[1250]	[2927]	0.645 ± 0.024	8	144
NaBr	$36\,155 \pm 90$	$24\,749 \pm 175$	[1250]	[2927]	0.661 ± 0.015	9	85
KCl	$37\,039 \pm 123$	$26\,049 \pm 215$	[1500]	[2927]	0.668 ± 0.025	9	116
NaCl	$37\,138 \pm 127$	$28\,559 \pm 224$	[1500]	[2927]	0.673 ± 0.025	9	120
KI	$34\,614 \pm 81$	$18\,367 \pm 522$	[1050]	2808 \pm 81	0.562 ± 0.039	6	217
NaI	$34\,251 \pm 98$	$19\,903 \pm 845$	[1050]	[2808]	0.583 ± 0.038	6	194

larger than those for a 4f electron. A lanthanide ion in the hosts considered in this work sits at the center of an octahedron composed of near negative ion neighbors. The splitting of the 5d orbital can be described by the parameter $B^4(\text{dd})$, the coefficient of $C_0^{(4)} + (5/14)^{1/2}(C_4^{(4)} + C_{-4}^{(4)})$ which is equivalent to $21 Dq$ or $2.1[E(5d e_g) - E(5d t_{2g})]$. The 4f orbitals are also subject to crystal-field splitting, but this is much weaker than that for the 5d orbitals and has little impact on the calculated f–d spectra. The parameters can be taken from the $4f^{13}$ configuration of Yb^{3+} ions in other hosts with the same ligands (in both atom type and structure) [22–25] as an approximation. The values adopted are listed in table 3.

3.2. The reduction of free ion parameters due to the nephelauxetic effect

Apart from the crystal-field splitting, 5d orbitals can also mix with orbitals from ligand ions which have much smaller overlap with 4f orbitals and hence reduce the strength of effective Coulomb interaction parameters. Such mixing also reduces the effective spin–orbit interaction parameters for the mixed 5d orbitals. Hence we introduce two parameters to describe the mixing:

$$|t_{2g}\rangle = \left(1 + |C_{t_{2g}}|^2\right)^{-\frac{1}{2}} \left(|5d, t_{2g}\rangle + C_{t_{2g}} |\text{ligand}, t_{2g}\rangle\right),$$

$$|e_g\rangle = \left(1 + |C_{e_g}|^2\right)^{-\frac{1}{2}} \left(|5d, e_g\rangle + C_{e_g} |\text{ligand}, e_g\rangle\right)$$

where $|\text{ligand}, t_{2g}\rangle$ and $|\text{ligand}, e_g\rangle$ are normalized wavefunctions describing the contributions to $|t_{2g}\rangle$ and $|e_g\rangle$ single-electron orbitals, respectively, from ligand ions, and $C_{t_{2g}}$ and C_{e_g} the corresponding coefficients. In general $C_{t_{2g}}$ can be different from C_{e_g} but here the difference is neglected by setting $C_{t_{2g}} = C_{e_g} = C$ for simplicity and reduction of number of parameters.

In order to simplify the calculation further, we also neglect the small overlap between 4f and orbitals from ligands and the Coulomb interaction and spin–orbit interaction between ligand orbitals.

With the above approximations, the interactions in the $4f^{13}(|t_{2g}\rangle + |e_g\rangle)$ configuration have exactly the same form as the pure $4f^{13}5d$ configuration, except that both the Coulomb interaction between 4f and ‘5d’, and the spin–orbit interaction for ‘5d’ are reduced by multiplying a factor of $\eta = (1 + C^2)^{-1}$. The nephelauxetic effect on spin–orbit interaction for 4f orbitals is expected to be small and so the free ion parameter value can be used for the ion in crystals.

3.3. Calculation results

The energy levels of Yb^{2+} in KF, KCl, KBr, KI, NaCl, NaBr and NaI were measured and simulated by Bland and Smith [17] and Tsuboi *et al* [19]. However, the crystal-field parameters for 4f electrons given seem to be an order of magnitude too small compared to Yb^{3+} in the elpasolite lattice, which has exactly the same ligands but only a slightly different bond length. A repeated calculation using the parameters presented in [17] gives a set of energy levels totally different from those presented in that publication. A fitting to the calculated T_{1u} energy levels presented in [17] turns out to be almost perfect, in that the residue is as small as the rounding error. However, the crystal-field parameters turn out to be negative rather than positive, and hence of the wrong sign.

Herein, the least squares fitting of the measured energy levels in [17, 19] using only three variable parameters E_{exc} , $B^4(\text{dd})$, and the reduction factor η , with other parameters fixed at the values discussed above, has been carried out. It is noted that the residual error of $\sim 100 \text{ cm}^{-1}$ is comparable with the uncertainty of the measured energies. For NaI and KI the residuals can be reduced from ca 300 to ca 200 cm^{-1} by letting ζ_{4f} vary. The parameters obtained are given in table 3. The absorption spectra for all the seven systems are well simulated from the calculated energy levels using the calculated relative electric dipole oscillator strengths (with no parameters being involved). The absorption spectrum for KCl: Yb^{2+} is plotted in figure 2 (the one with $B^{2f} = 0$).

The previously unexplained extra bands E_1 at 34 000 cm^{-1} and E_2 at 44 000 cm^{-1} in KCl [17] (at slightly different energies in other hosts) can be naturally explained as due to $4f^{14}-4f^{13}6s$ absorptions, which shift slightly to lower energy in various hosts relative to those in the free ion and become partially electric dipole allowed through mixing with $4f^{13}5d$ levels.

It is evident that all the parameters are reasonably well defined and there is a clear trend of decreasing E_{exc} , $B^4(\text{dd})$ and η values with the decreasing ionicity of ligands in the order $\text{F}^- > \text{Cl}^- > \text{Br}^- > \text{I}^-$. For hosts with the same ligands but different cations, the difference in parameter values are much smaller. This can serve as a guideline for determining the energy level parameters for lanthanide ions in other hosts.

4. The effect of the charge compensation on the crystal-field interaction

The effect of charge compensation is neglected in the above calculation. Due to the difference in charge on K^+ and Yb^{2+}

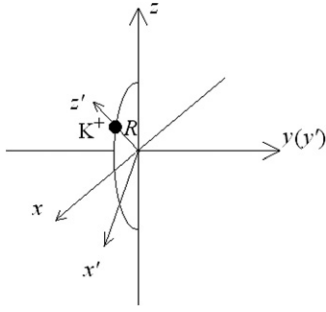


Figure 1. The relation between the coordinate frame xyz for O_h symmetry and $x'y'z'$ for C_{2v} symmetry. The xyz frame is so chosen that the y and y' axes are coincident and z' is the diagonal of the xz axes.

(we consider the case of KCl without loss of generality) there will be a charge compensation vacancy and the total energy of the system favors a vacancy at the nearest cation site. With such a vacancy at the second nearest neighbor, the site symmetry of Yb^{2+} reduces to C_{2v} . It is reasonable to believe that the distortion of the lattice due to low concentration doping of Yb^{2+} and cation-ion charge compensation is negligible. The crystal-field Hamiltonian $H_{cf}(C_{2v})$ deviates from the octahedral crystal-field Hamiltonian $H_{cf}(O_h)$ by taking the effect of mixing K^+ into account, i.e.:

$$H_{cf}(C_{2v}) = H_{cf}(O_h) - H_{cf}(K^+).$$

The crystal-field interaction is actually an effective interaction rather than only the anisotropic interaction on the 4f or 5d electron due to point charge from the lattice. Many theoretical studies have been carried out to explore the mechanism of this effective interaction. Here we can separate the contributions to crystal-field interactions into two parts. One part is due to charges and electric polarizations of all the ions from the lattice, which is of long range, and the other part is due to the covalent effect, i.e., the overlapping of 4f (or 5d) orbitals with those of the ligands, which is of short range. It is reasonable to assume that the introduction of a vacancy at the second nearest neighbor position does not effect the arrangement of nearest neighbors of Yb^{2+} ions, and $H_{cf}(K^+)$ contains only contributions due to the charge of K^+ .

In order to calculate the crystal-field interaction, we use the coordinate frame xyz shown in figure 1, where x , y , and z are the three four-fold rotational axes of O_h symmetry, and the plane with K^+ vacancy is chosen as the $x-z$ plane. Another coordinate frame $x'y'z'$ is chosen so that K^+ is on the z' axis. The contribution to the crystal-field Hamiltonian due to the charge K^+ , i.e., $H_{cf}(K^+)$, can be written as spherical tensors with coordinates for $x'y'z'$ frame as:

$$H_{cf}(K^+) = \frac{-e^2 \langle r^2 \rangle}{\epsilon R^3} C_0^2(\theta', \varphi') + \frac{-e^2 \langle r^4 \rangle}{\epsilon R^5} C_0^4(\theta', \varphi') + \frac{-e^2 \langle r^6 \rangle}{\epsilon R^7} C_0^6(\theta', \varphi'),$$

where $\langle r^k \rangle$ ($k = 2, 4, 6$) are the appropriate radial integrals, and ϵ is an effective dielectric factor to take the charge screening effect into account. Since $H_{cf}(K^+)$ itself is a small term

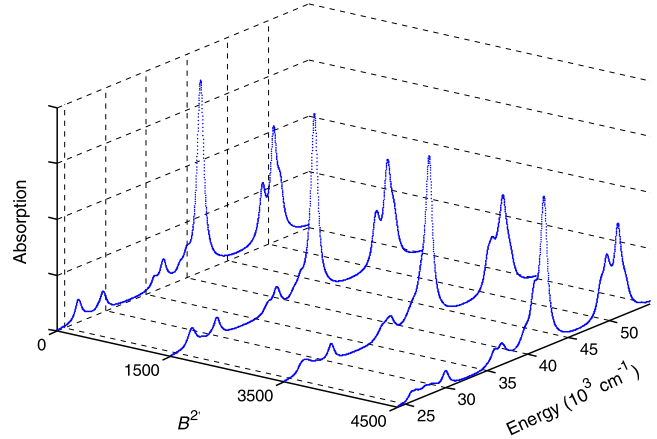


Figure 2. Variation of calculated KCl:Yb²⁺ absorption spectrum with the strength of the crystal-field parameter B^2 .

(This figure is in colour only in the electronic version)

already, we neglect the rank 4 and 6 terms in $H_{cf}(K^+)$ that have much smaller crystal-field coefficients. The rank 2 term can be expressed with spherical tensors with variables for the xyz frame as:

$$H_{cf}(K^+) \approx -B_0^2 \left[\frac{1}{4} C_0^2(\theta, \varphi) + \frac{\sqrt{6}}{8} (C_2^2(\theta, \varphi) + C_{-2}^2(\theta, \varphi)) - \frac{\sqrt{6}}{4} (C_1^2(\theta, \varphi) - C_{-1}^2(\theta, \varphi)) \right],$$

where $B_0^2 = \frac{e^2 \langle r^2 \rangle}{\epsilon R^3}$ can be either calculated or treated as an adjustable parameter. *Ab initio* calculations give $\langle r^2 \rangle_{4f} = 1.9 \times 10^{-21} \text{ m}^2$, and $\langle r^2 \rangle_{5d} = 1.3 \times 10^{-20} \text{ m}^2$. Using $R = 4 \times 10^{-10} \text{ m}$ and $\epsilon = 5.9$ (the static dielectric factor for NaCl), we obtain $B_0^2(4f) = 230 \text{ cm}^{-1}$ and $B_0^2(5d) = 1600 \text{ cm}^{-1}$. Since $B_0^2(4f)$ is much smaller than $B_0^2(5d)$, we neglect the former and calculate the effect of the latter upon the absorption spectra and the lowest few energy levels that affect the emission lifetimes relevant to the two emission bands.

These two emission bands I, II have an energy gap between them of roughly 2000 cm^{-1} or 10 phonons, similar to the case of $\text{SrCl}_2:\text{Yb}^{2+}$ [16]. The energy levels that contribute to the emissions are calculated and tabulated in table 4 for the two cases without and with the effect of the K^+ vacancy (i.e. O_h and C_{2v} symmetry) being taken into account.

For the case without considering the effect of the K^+ vacancy, the band with lower energy (II) is related to the initial states of one E_u and one T_{2u} level, whose emission to the single ground state are both electric dipole forbidden; and the band with higher energy (I) is composed of emission from several energy levels, with the emission from the lowest two (26430 and 26597 cm^{-1}) being electric dipole forbidden and from the third level (26630 cm^{-1}) being strongly electric dipole allowed. Calculations show that the relative positions of those levels only vary slightly for quite a wide range of parameters. From those energy levels for O_h symmetry, the radiative lifetime of the electric dipole forbidden lower energy band is predicted to be similar to the case of $\text{SrCl}_2:\text{Yb}^{2+}$ [16], i.e., of the order of magnitude of 1 ms, while the radiative lifetime of

Table 4. The calculated levels that give the two emission bands in the spectra of Yb^{2+} . $\langle 4f|r|5d \rangle = 0.0253$ nm is taken from the many-body perturbation calculation [26]. Energies are in the unit of cm^{-1} ; line strengths ($\sum_{i,f,q} |\langle Ff| -r C_q^{(1)} |Ii \rangle|^2 / 3$) are in units of 10^{-20}cm^2 ; blanks in the line strength column indicate forbidden transitions. From O_h to C_{2v} , energy levels not only split but also cross.

Band	No.	Irrep	O_h		C_{2v}			
			Energy	Line strength	Energy	Line strength		
II	1	E	24 469		24 329			
	2				24 350	0.002		
	3				244 94	0.027		
	4	T_2			24 515	0.044		
	5				24 579			
I	6	T_2	26 430	79.4	26 249	9.5		
	7				26 311			
	8				26 320	0.9		
	9	E			26 597	26 323	12.4	
	10				26 557	5.1		
	11	T_1			26 582	6.3		
	12				26 642	8.5		
	13				26 644	0		
	14	A_2			26 699	26 651	13.7	
	15				26 673	7.4		
	16	T_1			26 775	6.3	26 722	4.4
	17				26 760	0		
	18	T_2			26 802	26 848	7.8	
	19				26 863	2.2		
	20				26 911	3.3		
	21	T_1			27 039	6.2	27 054	0.03
	22				27 084	5.6		
	23				27 143	2.8		
	24				A_1	27 171	27 160	
Total		91.9		90.0				

the higher energy band is predicted to vary dramatically from the order of magnitude of 1 ms at very low temperature to the order of 1 μs (assuming thermal balance between energy levels in the range 26 430–27 171 cm^{-1}).

For the case with the effect of K^+ vacancy considered, the groups of energy levels for the lower energy band split into 5 nondegenerate levels, the middle three of which are partially electric dipole allowed due to their mixing with higher states which are electric dipole allowed even at the O_h approximation. This can shorten the radiative lifetime of the lower energy band dramatically from the order of magnitude of ms at low temperature to hundreds of μs at room temperature (estimated by assuming thermal equilibrium between the five levels in this band). The groups of energy levels for the higher energy band split into 19 nondegenerate levels with distributive electric dipole strength. By assuming thermal equilibrium between those levels, the radiative emission lifetime is expected to vary smoothly at ca μs when the temperature varies.

There is no experimental measurement of the lifetime of $\text{KCl}:\text{Yb}^{2+}$, but it is expected that the lifetime should be quite similar to the case $\text{NaCl}:\text{Yb}^{2+}$ reported by Tsuboi *et al* [19], which agrees qualitatively with the above calculation with the effect of K^+ vacancy included.

In order to see the effect of the K^+ vacancy to the absorption spectra, we have calculated absorption spectra with $B_0^2(5d) = 0, 1500, 3000$ and 4500cm^{-1} and the results are plotted in figure 2. Hardly any difference can be seen between the spectra with $B_0^2(5d) = 0$ and 1500cm^{-1} . The spectrum with $B_0^2(5d) = 3000 \text{cm}^{-1}$ is still very close

to the measured absorption spectrum. Only the spectrum with $B_0^2(5d) = 4500 \text{cm}^{-1}$ is noticeably different from the measured absorption spectrum and from the calculated ones with smaller $B_0^2(5d)$. This justifies why the deviation from O_h symmetry due to a cation vacancy at second nearest neighbor can be safely neglected in the simulation of absorption spectra.

5. Conclusions

This theoretical study has rationalized the absorption spectra of Yb^{2+} in alkali halide matrices by utilizing very few adjustable parameters. Moreover, the effects of charge compensation in these systems have been considered. Although the inclusion of charge compensation into the modeling of the absorption spectra has little effect, it is shown to be important when simulating the luminescence dynamics of these systems.

Acknowledgments

Financial support for this study is acknowledged under the City University Research Grant 9360123 and the National Natural Science Foundation of China Grant No. 10704090.

References

- [1] Wegh R T, Donker H, Oskam K D and Meijerink A 1999 *Science* **283** 663
- [2] Liu X M and Lin J 2008 *J. Mater. Chem.* **18** 221
- [3] Liu X M and Lin J 2007 *Appl. Phys. Lett.* **90** 184108

- [4] Lin J, Yu M, Lin C K and Liu X M 2007 *J. Phys. Chem. C* **111** 5835
- [5] Yu M, Lin J and Fang J Y 2005 *Chem. Mater.* **17** 1783
- [6] Rubio O J 1991 *J. Phys. Chem. Solids* **52** 101
- [7] Carnall W T, Goodman G L, Rajnak K and Rana R S 1989 *J. Chem. Phys.* **90** 3443
- [8] van Pieterse L, Reid M F, Burdick G W and Meijerink A 2002 *Phys. Rev. B* **65** 045114
- [9] Dorenbos P 2003 *J. Phys.: Condens. Matter* **15** 575
- [10] Dorenbos P 2000 *J. Lumin.* **91** 155
- [11] Dorenbos P 2000 *J. Lumin.* **91** 91
- [12] Dorenbos P 2002 *J. Alloys Compounds* **341** 156
- [13] Duan C K and Reid M F 2003 *J. Solid State Chem.* **171** 299
- [14] Xia S D and Duan C K 2007 *J. Lumin.* **122** 1
- [15] Reid M F, van Pieterse L, Wegh R T and Meijerink A 2000 *Phys. Rev. B* **62** 014749
- [16] Pan Z F, Duan C K and Tanner P A 2008 *Phys. Rev. B* **77** 085114
- [17] Bland S W and Smith M J A 1985 *J. Phys. C: Solid State Phys.* **18** 1525
- [18] Tsuboi T, Witzke H and McClure D S 1981 *J. Lumin.* **24/25** 305
- [19] Tsuboi T, McClure D S and Wong W C 1993 *Phys. Rev. B* **48** 62
- [20] Öberg K J and Lundberg H 2007 *Eur. Phys. J. D* **42** 15
- [21] Cowan R D 1981 *The Theory of Atomic Structure and Spectra* (Berkeley, CA: University of California)
- [22] Tanner P A, Ravi Kanth Kumar V, Jayasankar C K and Reid M F 1994 *J. Alloys Compounds* **215** 349
- [23] Zhou X J, Reid M F, Faucher M D and Tanner P A 2006 *J. Phys. Chem. B* **110** 14939
- [24] Reid M F and Richardson F S 1985 *J. Chem. Phys.* **83** 3831
- [25] Tanner P A, Mak C S K, Edelstein N M, Murdoch K M, Liu G K, Huang J, Seijo L and Barandiaran Z 2003 *J. Am. Chem. Soc.* **125** 13225
- [26] Chen T, Duan C K and Xia S D 2007 *J. Alloys Compounds* **439** 363